ACS APPLIED MATERIALS & INTERFACES

Research Article

www.acsami.org

Flexible Palladium-Based H_2 Sensor with Fast Response and Low Leakage Detection by Nanoimprint Lithography

Su Hui Lim,[†,‡] Boya Radha,*[,†,§,∥] Jie Yong Chan,[‡] Mohammad S. M. Saifullah,*[,†] Giridhar U. Kulkarni,*[,§] and Ghim Wei Ho*[,‡]

[†]Institute of Materials Research and Engineering, A*STAR (Agency for Science, Technology and Research), 3 Research Link, Singapore 117602, Republic of Singapore

[‡]Department of Electrical and Computer Engineering, National University of Singapore, 21 Lower Kent Ridge Road, Singapore 117576, Republic of Singapore

[§]Chemistry and Physics of Materials Unit and DST Unit on Nanoscience, Jawaharlal Nehru Centre for Advanced Scientific Research, Jakkur P.O., Bangalore -560064, India

Supporting Information

ABSTRACT: Flexible palladium-based H_2 sensors have a great potential in advanced sensing applications, as they offer advantages such as light weight, space conservation, and mechanical durability. Despite these advantages, the paucity of such sensors is due to the fact that they are difficult to fabricate while maintaining excellent sensing performance. Here, we demonstrate, using direct nanoimprint lithography of palladium, the fabrication of a flexible, durable, and fast responsive H_2 sensor that is capable of detecting H_2 gas concentration as low as 50 ppm. High resolution and high throughput patterning of palladium gratings over a 2 cm × 1 cm area on a rigid substrate was achieved by heat-treating nanoimprinted palladium benzyl mercaptide at 250 °C for 1 h. The flexible and robust H_2 sensing device was fabricated by subsequent transfer nanoimprinting of these gratings into a polycarbonate film at its glass transition temperature. This technique produces flexible H_2 sensors with improved durability, sensitivity, and response time in comparison to palladium thin films. At ambient pressure and temperature, the device showed a fast response time of 18 s at a H_2 concentration of 3500 ppm. At 50 ppm concentration, the response time was found to be 57 s. The flexibility of the sensor does not appear to compromise its performance.

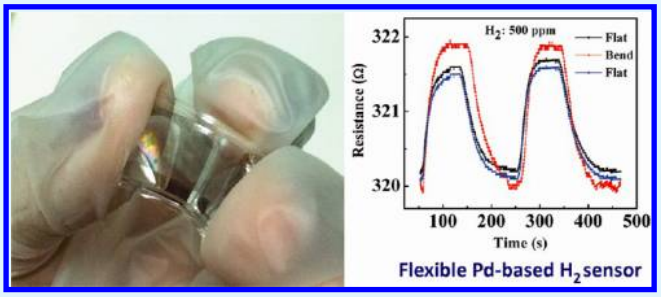

KEYWORDS: *nanoimprint lithography, palladium, hydrogen, sensing, flexible sensor, patterning*

INTRODUCTION

Hyrogen (H_2), being a clean, affordable, and reliable source of energy, has found wide-ranging applications not only in propulsion systems, fuel cells, and H_2-fuelled cars but also as a feedstock in a variety of chemical, industrial, and metallurgical processes. However, H_2, a colorless and odorless gas, is highly flammable and becomes explosive when its concentration exceeds 4% in air.[1] This makes safety a critical aspect in hydrogen economy. For this reason, fast, affordable, and reliable detection of H_2 gas is required for furthering H_2-based applications.

Palladium (Pd) is widely used as a sensing material for H_2 due to its ability to absorb up to 900 times its own volume of H_2 at room temperature and atmospheric pressure. When Pd is exposed to H_2 gas, the gas molecules are adsorbed onto the metal surface and dissociates into hydrogen atoms.[2] Bulk diffusion of these hydrogen atoms *via* grain boundaries, dislocations, and other defects lead to the occupation of interstitial sites of the Pd lattice. This effectuates certain amount of lattice expansion.[2,3] Absorbed hydrogen converts Pd into Pd hydride.[4,5] At low concentrations of H_2 (up to ∼200 ppm), occupation of lattice structure causes it to expand slightly and this leads to α-hydride formation. At concentrations of ∼1000 ppm, the α-hydride phase starts to convert to the β-phase, and this is associated with an even larger lattice expansion. At concentrations higher than 5500 ppm, all of the α-phase would have disappeared, leaving only the β-phase Pd hydride.[6] The formation of hydrides gives rise to increased frequency of scattering events of charge carriers, which, in turn, directly leads to the increase of electrical resistance in Pd—the magnitude of which is directly proportional to the atomic fraction of absorbed hydrogen atoms to Pd atoms.[6] Another accompanying effect due to the formation of Pd hydride is the change in optical property of the material leading to differences in path length, transmittance, reflectivity, etc.[7−10] An associated volume expansion, a change in the electrical resistance and

Received: May 1, 2013
Accepted: July 2, 2013
Published: July 2, 2013

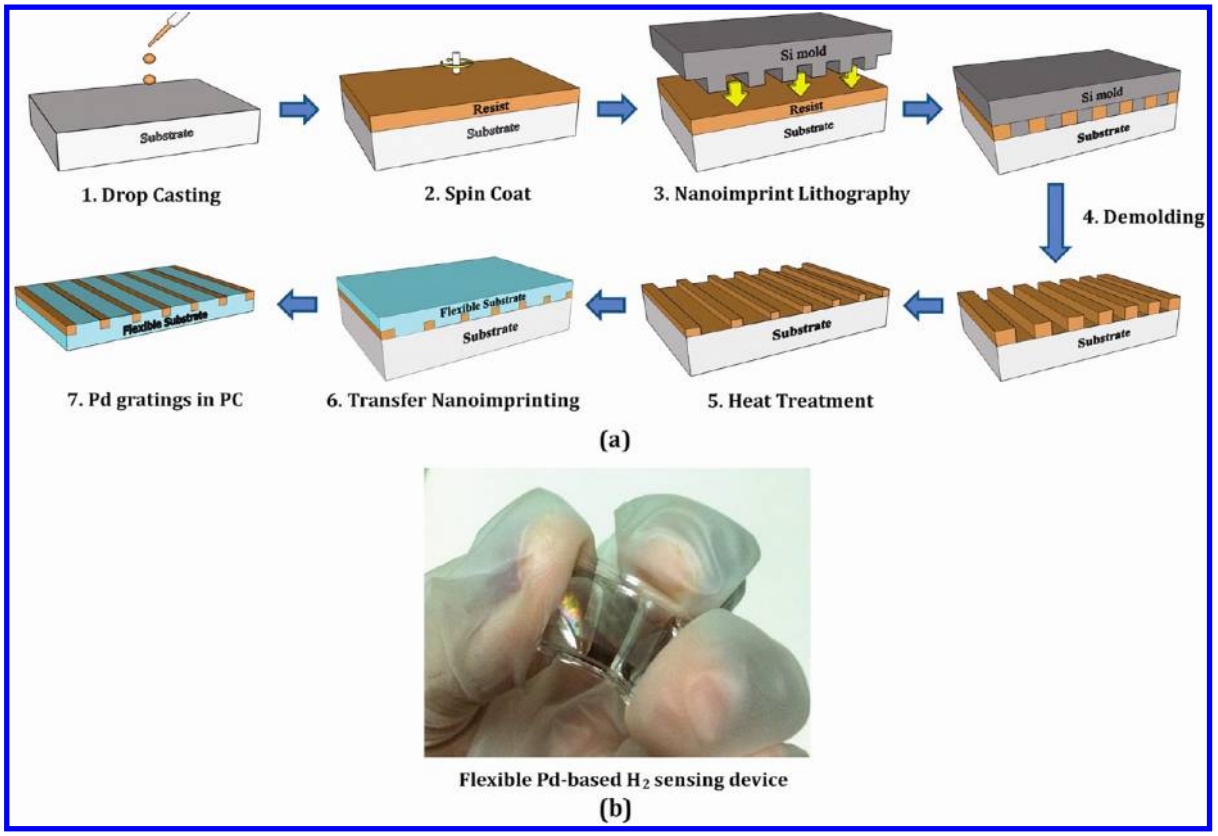

Figure 1. (a) Schematic illustration of the steps involved in the fabrication of a flexible Pd-based H_2 sensor by nanoimprint lithography. (b) A flexible sensor with slightly translucent patterned area of 2 cm × 1 cm containing Pd lines in a clear PC film of size 3 cm × 2 cm.

optical properties during conversion to Pd hydride are used as sensing strategies to detect H_2 gas. However, many H_2 gas sensors utilize a combination of two of these three strategies. A popular mechanism of sensing involves using resistance increase upon influx of hydrogen leading to Pd hydride formation which mainly occurs on the surface of a Pd thin film.[5,11] However, in discontinuous Pd structures with nanogaps, H_2 absorption leads to swelling that improves electrical continuity thus *reducing* resistance. Favier et al. demonstrated the concept of nanogaps known as break junctions with electrodeposited Pd mesowires.[12] Recently, Lee et al. have shown the fabrication of lithography-free nanogap sensors based on a flexible PDMS substrate and also highlighted the motivation toward simple sensor fabrication for mass production.[13] A recent work by Greco et al. has also shown the possibility of using mixed resistive behavior to achieve H_2 gas sensing.[14]

In contrast to making nanogaps, thin film is an easy and low-cost option for the development of Pd-based H_2 sensors to overcome scalability problems associated with sophisticated nanogap patterning. Comparing the H_2 sensing performance of Pd nanostructures with bulk, the former allows an increased surface area-to-volume ratio, which increases the sensing performance of H_2 gas.[10,15−17] The fabrication of desirable nanostructures for sensing application using simple and scalable method is potentially challenging. With recent developments in nanotechnology, researchers have looked into controlling the morphology of Pd nanostructures. Many different nanostructures of Pd have been reported, including thin films,[11,18,19] nanoparticles,[20−24] nanolines,[25−29] nanotubes,[30,31] nanourchins,[32] etc.

Although nanostructuring increases the surface area, the accessibility of Pd nanostructures to H_2 is best achievable by surface patterning. Conventionally, Pd nanostructures are fabricated by lithography, and it involves many steps such as patterning of resist, metal deposition, etching, and lift-off. The fabrication of Pd nanostructures for H_2 gas sensing has also been demonstrated by electron beam lithography.[26,28] The smaller the Pd feature size and higher the surface area, the better will be the performance of the H_2 sensor. Topographic features with higher resolution demand sophisticated fabrication process and are generally limited by the overall area of the sensor device. The limitation is also in terms of being adaptable to flexible substrates. Among various nanopatterning techniques, nanoimprint lithography (NIL), foreseen as one of the next generation lithography techniques, holds the key to the fabrication process flexibility in terms of substrate materials, shape of structures, feature sizes, and resist materials.[33−37]

Flexible sensors are advantageous when they can simply be laminated around the pipelines for detecting leakage in chemical industries and in advanced applications such as fuel cell-powered vehicles and space shuttles. Pd-based resistive H_2 gas sensors are environmentally benign, have predictable response with increasing gas concentration, and draw minimal power. Flexible Pd-based sensors are intended to have good sensor performance in being compact and durable. We chose thin films and NIL as our fabrication methods as both are proven to be easily scalable to industrial scale. With these guidelines, Pd-based sensors were fabricated and tested in terms of response time, sensitivity at H_2 detection limits, and recovery. In this paper, we demonstrate the fabrication of a flexible Pd-based H_2 sensor in three steps: direct NIL of

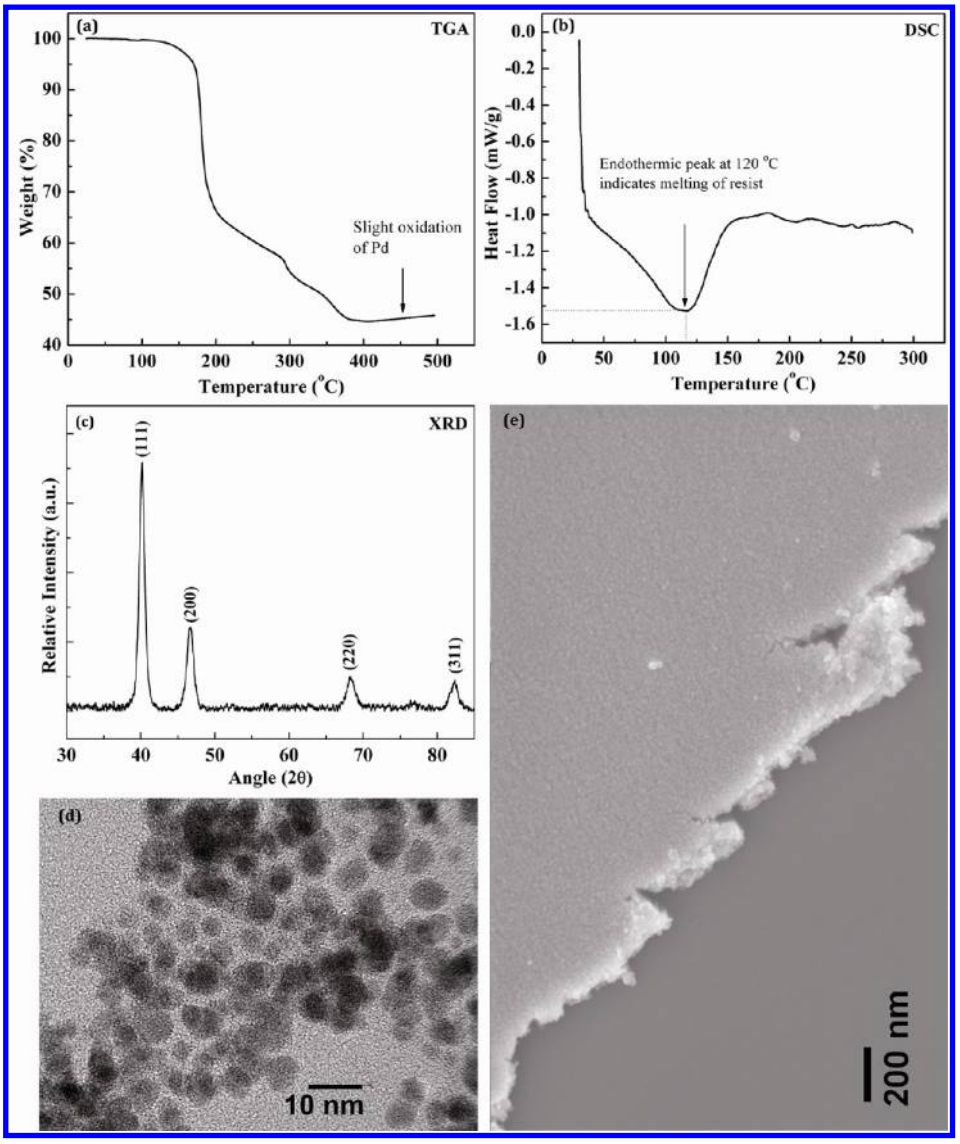

Figure 2. (a) TGA analysis of Pd benzyl mercaptide (PBM) in air from 25 to 500 °C. Major weight loss of 55% contributed to organic burnoff during heating. (b) DSC analysis of PBM from 0 to 300 °C. An endothermic peak at ~120 °C suggests melting of this compound. (c) X-ray diffraction pattern of the Pd thin films thermolyzed at 250 °C. (d) TEM and (e) SEM images of the Pd nanoparticles present in the film.

palladium benzyl mercaptide (PBM), a single source palladium precursor, on a rigid substrate of 2 cm × 1 cm area; its heat-treatment at 250 °C for 1 h to obtain Pd gratings; and, finally, transfer nanoimprinting of these structures into a polycarbonate film to obtain a flexible sensor. The sensor process fabrication throughput is greatly improved by employing a PBM single source precursor ink as it reduces the number of process steps. In addition, the chosen "imprint ink" (i.e., PBM) allows Pd patterning directly on either rigid or flexible substrates (Figure 1a).

■ RESULTS AND DISCUSSION

PBM forms smooth films upon spin coating and can easily be converted to metallic Pd by a simple thermolysis step in air at 250 °C. Another important characteristic of this compound is that it melts at a temperature as low as 120 °C.[37] This enables the material to flow easily into the features of the mold and thus can be utilized as an "imprint ink" for successful nanoimprinting. We have called this process as direct metal nanoimprint lithography (DM-NIL), as the imprinted precursor can be directly converted to Pd metal after thermolysis. TGA and DSC studies of PBM were carried out to understand its weight loss behavior and to identify the melting endotherm, respectively. The TGA showed a weight loss resulting in residue of ~45% beyond 300 °C, which corresponds closely to stoichiometric amount of Pd in the precursor (Figure 2a and Supporting Information). Further increase in temperature resulted in the slight oxidation of Pd. In order to avoid surface oxidation, the decomposition was conducted under isothermal condition at a reduced temperature of 250 °C. The DSC showed an endothermic peak at ~120 °C, and this was due to the melting of PBM (Figure 2b).

The PBM film, on heating at 250 °C for 1 h, resulted in the formation Pd thin film. This was verified by the presence of only Pd peaks in the XRD pattern (JCPDS Card No. 46-1043) after thermolysis (Figure 2c). The average grain size of the film was estimated from the full width at half-maximum of (111) peak and gave a value of L_{111} = 11 ± 0.1 nm. Composition analysis was also done by X-ray photoelectron spectroscopy, which showed the amount of carbon to be ~20 atom % (see

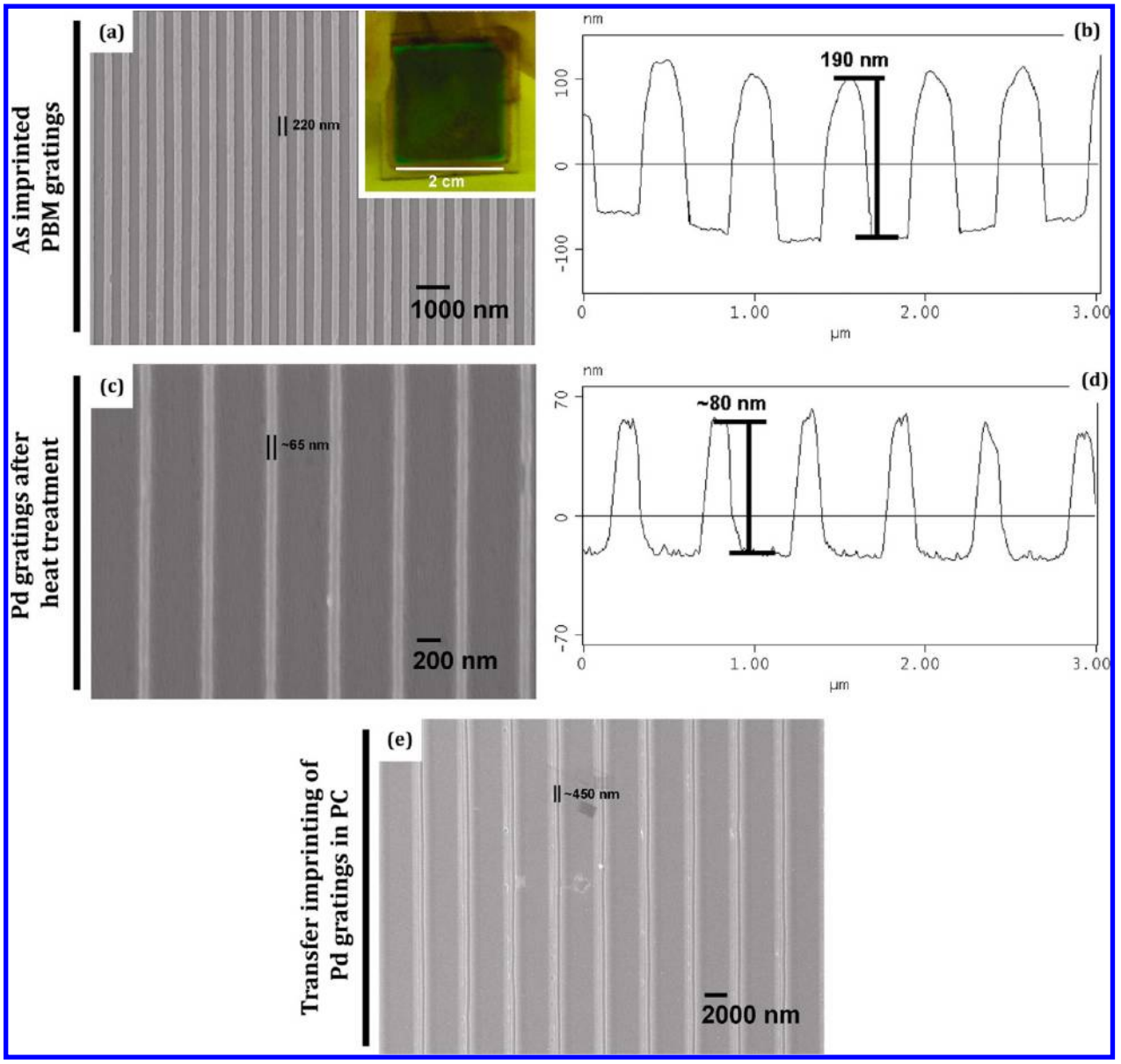

Figure 3. (a) SEM and (b) AFM images of the 250 nm wide as imprinted PBM structures on glass. Inset in part a shows uniform patterning of gratings over a large area of 2 cm × 2 cm. Heat treatment of the imprinted structure gives Pd gratings whose width and height are seen in the (c) SEM and (d) AFM images, respectively. (e) Flexible sensor was fabricated by transfer imprinting of slightly wider Pd gratings into polycarbonate sheets. Metallic gold was deposited on the flexible sensor to facilitate imaging.

the Supporting Information). The TEM image showed the particle size, which on an average, was less than 10 nm (Figure 2d). Figure 2e shows a SEM image of the heat treated Pd film revealing that the film comprised of densely packed Pd nanoparticles (average surface roughness, ∼1.7 nm, see the Supporting Information). The nanoparticlulate film is advantageous, as it allows higher H_2 diffusion and thus better sensing due to higher surface area.[38]

To test the hypothesis whether the sensitivity and response time of the H_2 sensor can be enhanced by increasing the surface area by nanostructuring as compared to the thin films, Pd gratings were patterned by DM-NIL. A Si mold containing 250 nm grating structures was used to imprint PBM film at a temperature of 120 °C and pressure of 50 bar for 10 min. Upon melting, the precursor ink flowed into the channels of Si mold and replicated the features of the mold on the substrate. This is analogous to the well-established patterning of conventional polymers by NIL where the polymer being imprinted is taken through the glass transition temperature (T_g). The setup was cooled to room temperature and demolded to achieve PBM patterns on a glass substrate (Figure 3a and b). The inset in Figure 3a shows 220 nm wide PBM lines obtained on the substrate over an area of 2 cm × 2 cm. Upon isothermal heat-treatment at 250 °C for 1 h, Pd nanolines of width ∼65 nm and height ∼80 nm were obtained (Figure 3c and d). The heat treatment resulted in shrinkage of imprinted grating structures to ∼70% and 60% of the original size laterally and vertically, respectively, due to the loss of organics during thermolysis. The metal residual layer leads to electrical continuity of the Pd nanolines in parallel as well as perpendicular directions. The thin residual layer may or may not be required, depending upon the final use of the imprinted structure. In the present case, the residual layer was left intact, as it also served the purpose of providing electrical continuity. The thickness of residual layer

dx.doi.org/10.1021/am401624r | ACS Appl. Mater. Interfaces 2013, 5, 7274−7281

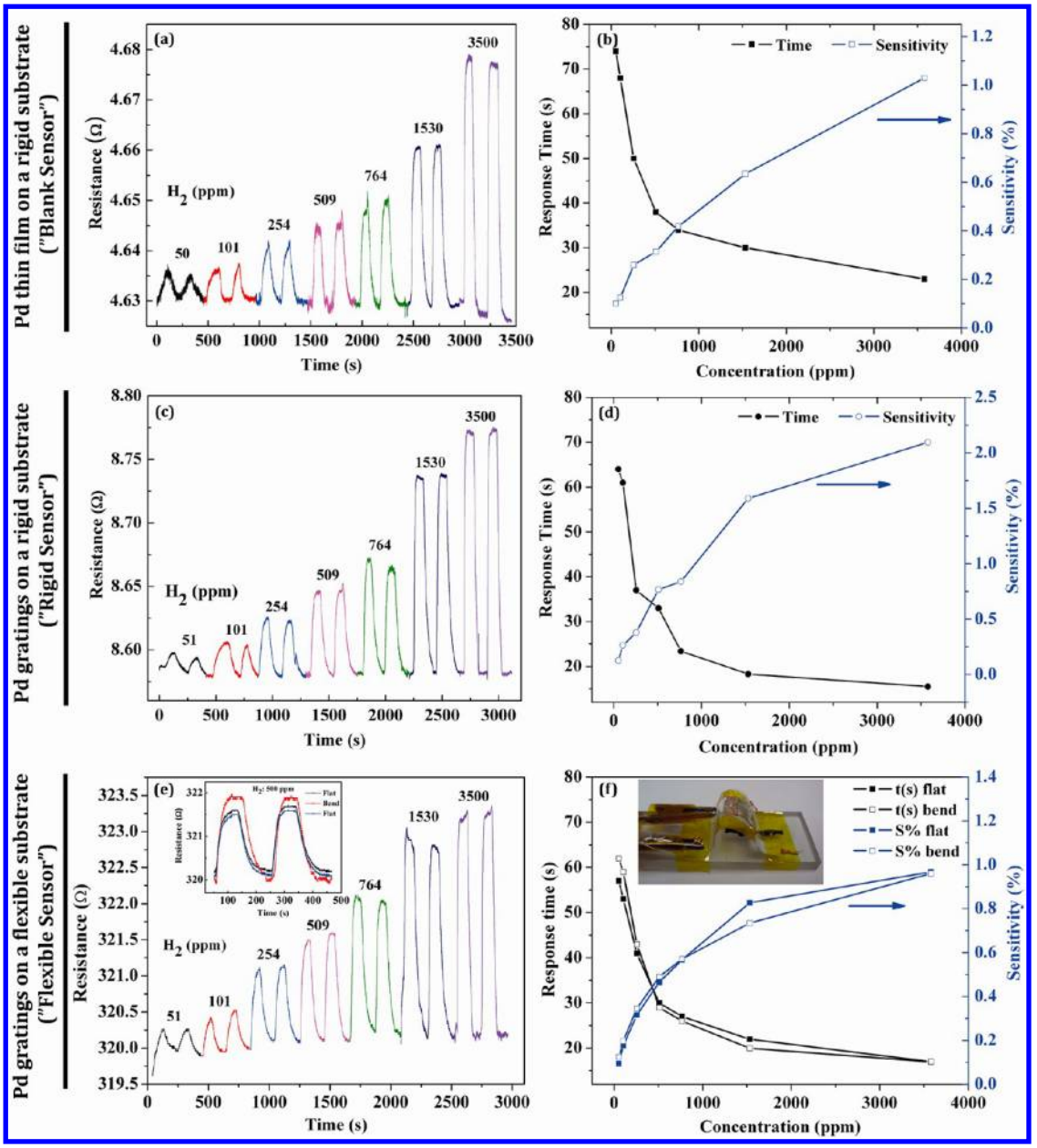

Figure 4. Real-time electrical resistance response to H_2 within a concentration range of 50−3500 ppm at room temperature of (a) blank, (c) rigid, and (e) flexible sensors. Response time and sensitivity as a function of H_2 concentration of (b) blank, (d) rigid, and (e) flexible sensors. Inset in part e shows the response curve of the flexible sensor at a H_2 concentration of 500 ppm when the device was taken from flat to bent to again flat configuration. The inset in part f shows a flexible sensor bent at an angle of 90°.

was found to be ∼20−30 nm. The average roughness of the residual layer (1.73 ± 0.3 nm) was similar to that of Pd lines (2.41 ± 0.5 nm). The metal grating structures were used for H_2 sensing (or 'rigid sensor'), and its performance was compared with an unpatterned Pd film (or 'blank sensor') of thickness ∼97 nm. The blank sensor was prepared by thermolysis of spin-coated PBM film (250 °C for 1 h) on a glass substrate of 2 cm × 2 cm area.

Figure 4a represents the response curve for change in resistance of the blank sensor on a glass substrate recorded when H_2 flow (from 50 to 3500 ppm) was turned on and off for two cycles. For the case of higher H_2 concentration of ∼3500 ppm, the increase in resistance was very abrupt (∼23 s) and the device recovered quickly (within ∼39 s of Ar flush) with a decrease in resistance returning to its original value. However, at a lower concentration of ∼50 ppm, the change in resistance is more linear with time (∼75 s) and the recovery is very slow (∼82 s) due to less hydrogen accessibility. The device performance was evaluated by the sensitivity and response time. Sensitivity measures the change in physical or chemical properties of the sensor with respect to change in H_2 concentration. The response time, on the other hand, indicates the speed of change in property of the material when exposed to H_2 gas.[5] It is taken as the time needed for resistance of the sensor to reach 90% of the maximum resistance when H_2 gas is introduced into the chamber.[15] When H_2 concentration was decreased, the sensitivity decreased while the response time increased (Figure 4b). The shortest response time achieved using the blank device was 23 s at a H_2 concentration of 3500 ppm and at the lowest concentration of 50 ppm, a response

time of 75 s was obtained. As the concentration of H_2 reduced, the response time is much larger as the change in resistance is not very obvious. It is interesting to note that the change in response time is nearly exponential with the decrease in concentration of H_2 gas. A similar trend was observed in the case of sensitivity; at lower concentrations, the sensitivity was lower. For a Pd film-based H_2 sensor, at lower concentrations of H_2 gas such as 50 ppm, Pd hydride formation and in turn the device performance is expected to be sluggish. However, in our case, we obtained a relatively faster response time at low concentration, compared to sputtered Pd thin films[19] or electrochemically deposited Pd nanoparticles of approximately same size (see Supporting Information).[20,21] This may be attributed to the densely packed Pd nanoparticles enhancing the available surface area.

A survey of the scientific literature on Pd-based H_2 sensors suggests that fast response time is obtained with structured surfaces as opposed to films (see the Supporting Information). In line with the earlier literature, our patterned Pd H_2 sensing device on glass (i.e., the rigid sensor) showed the shortest response of ∼15 s at a concentration of 3500 ppm H_2 while it had a response time of ∼64 s at the lowest measured concentration of 50 ppm (Figure 4c and d), which is lower than the value observed for unpatterned thin film (∼75 s).

Thus far, we have discussed H_2 sensors on rigid substrates such as glass. Flexible sensors own many advantages over rigid sensors with their ability to be conformal over surfaces leading to less occupation of space. Although the former are currently not as widespread, they continue to challenge rigid sensors in cost and application niches. Flexible H_2 sensor was fabricated by transfer nanoimprinting Pd gratings on a rigid (glass) substrate to flexible PC substrate at its glass transition temperature using NIL (Figures 1b and 3e and f). This method of transfer nanoimprinting eliminates the high temperature processing (i.e., thermolysis of PBM at 250 °C) of flexible PC substrate, which paves way for generic transfer of any patterned features on rigid surfaces. As well-known in the literature, transferring nanostructures to soft rubbery poly(dimethylsiloxane) (PDMS) elastomer can be easily done by simple thermal curing of PDMS over the nanostructures. However, the nonrubbery, nonporous flexible substrates such as PC carrying sensing element provide an additional advantage of being impermeable to other gases. To increase the robustness of the sensing element, slightly wider (∼450 nm) Pd gratings were used. Figure 4e shows the responses recorded for two H_2 cycles, while the sensor was in flat-bend-flat configuration. The fabricated flexible H_2 sensor could sustain considerable amount of bending (bend angle ∼90°) during H_2 sensing (Figure 4f, inset). As evident, there is not much change in the response time and sensitivity despite subjecting the sensor to bending, indicating a good performance fidelity of the device. The mechanical durability of the flexible sensor was confirmed by performing H_2 sensing for the gas concentrations from 50 to 3500 ppm without any degradation in performance (Figure 4f). These results are very promising for practical applications demanding high mechanical durability of the device and its ability to conform the surface (Figure 1).

The comparison of sensitivity and response time for all the devices, viz., blank, rigid, and flexible sensors is shown in Figure 4b, d, and f. The rigid sensor showed a much better performance than the blank device in terms of sensitivity and response time. The increased availability of the surface area due to patterning resulted in higher uptake of H_2 gas in the rigid sensor as opposed to the blank device, thereby leading to its increased sensitivity. On the other hand, the response time, which depends on the resistance change response of the material, does not show a considerable change with surface patterning. The gratings in the flexible sensor, resembling long submicrometer metallic wires, were embedded inside PC on all the three sides except the exposed top surface,[37] thereby providing considerably less surface area for the accessibility of H_2 gas. Our results are in agreement with the study by Yang et al. who showed that nanowires are far better sensors than thin films.[29] The response of the flexible Pd sensor was consistent in the full concentration range of the H_2 tested even when the sensor was in a bent configuration (see Supporting Information). The sensing performance of flexible sensor being preserved at a bend angle of 90° (radius of curvature = 3.57 mm) is encouraging as such sensors can be laminated or simply folded onto a curved structure such as pipe carrying H_2 gas. It is worthwhile pointing out that the sensitivity and response time of the flexible sensor is similar regardless of whether it is in flat or bent configuration.

The advantages of DM-NIL for fabricating flexible H_2 sensors over other techniques are scalability, low temperature processing, cost-effective fabrication with fast response sensing capability. Our flexible H_2 sensing device works efficiently at room temperature with a fast response time of 18 s at 3500 ppm. At low H_2 concentration of 50 ppm, the response time was found to be 57 s. These are the lowest reported values for flexible sensors at low H_2 concentrations (see the Supporting Information).[13,20,31]

CONCLUSIONS

We have demonstrated a flexible Pd-based H_2 sensor fabricated using DM-NIL with 100% yield *via* low temperature processing. DM-NIL utilizes PBM, an imprintable single source precursor, which decomposes to metallic Pd when isothermally heat-treated at 250 °C for 1 h. This property was utilized to pattern Pd gratings on glass which were subsequently transfer imprinted into a PC film at its glass transition temperature to obtain the flexible H_2 sensor. This sensor exhibits fast response of 18 s for H_2 concentration of 3500 ppm and 57 s for 50 ppm. Its sensing characteristics were unaffected by mechanical bending. Our fabrication technique has the potential to allow high yield scale-up and mass production of flexible sensors for industrial applications. This is ideal, as a flexible H_2 sensor should be compact, sensitive, and durable with short response time, and, more importantly, easily fabricated, unlike commercial H_2 sensors, which are usually assembled on a rigid substrate.

EXPERIMENTAL SECTION

Preparation of Pd "Direct Imprint" Ink. The starting compounds, benzyl mercaptan and palladium(II) acetate, were purchased from Fluka and Alfa Aesar, respectively. The steps of synthesizing Pd "imprint ink" are as follows. An equimolar amount of benzyl mercaptan was mixed with a solution of Pd acetate in toluene (Sigma Aldrich). The mixture was stirred for 15 h. Unreacted Pd acetate residue and acetic acid were obtained as byproducts. The residue was settled by centrifugation. The supernatant was separated and subjected to low pressure distillation in a rotary evaporator to remove excess solvent. For further purification, the supernatant was washed with methanol to remove unreacted mercaptan and left to dry in a vacuum oven at room temperature for 12 h. The resultant material was a brown powder, termed further on as Pd benzyl mercaptide (PBM).

Nanoimprint Lithography of Pd. The PBM powder was dissolved in chloroform to the desired concentration (0.28 M) to make the Pd "imprint ink". This solution was filtered through a 0.2 μm pore size filter and drop casted onto a precleaned glass/Si substrate of dimensions slightly over 2 cm × 2 cm. It was spin-coated at a speed of 400 rpm to obtain ∼500 nm thick PBM film. Si molds possessing line gratings of width 250 nm (mold size: 2 cm × 2 cm) and 2 μm (mold size: 2 cm × 1 cm), both with an aspect ratio of 1, were used to imprint features on glass and silicon. The mold was placed on top of the film and imprinted at an elevated pressure (50 bar) and temperature (120 °C) for 10 min using an Obducat nanoimprinter (Obducat, Sweden). Prior to imprinting, the Si molds were cleaned and coated with antisticking self-assembly monolayer of 1*H*,1*H*,2*H*,2*H*-perfluorodecyltrichlorosilane to reduce their surface energy. This was to ensure that the mold can be easily demolded after imprinting, leaving behind the nanostructured PBM thin film. After imprinting, the patterned films were subsequently transferred to a Carbolite chamber furnace and baked at 250 °C for 1 h to remove all the organics, leaving behind Pd metal with negligible amount of impurities. For the fabrication of flexible Pd sensors, Pd grating structures on a rigid substrate were transferred to a flexible polycarbonate (PC) substrate. This was done by transfer NIL where PC was employed as substrate (size: 3 cm × 2 cm, thickness: 125 μm) and patterned Pd on Si as mold. Under pressure (50 bar), the PC substrate was taken through T_g (∼140 °C) for 10 min, with Pd lines on top. After demolding, the PC substrate carried the Pd nanolines. The obtained yield was estimated optically to be ∼100%.

Characterization. The crystallinity of the Pd film was characterized using an X-ray diffractometer (Bruker D8 General Area Detector Diffraction System). A JEOL-JSM6700F field-emission scanning electron microscope (FE-SEM) and Nanoscope IV multimode atomic force microscope (AFM) were used to study the morphology and nanostructure of the Pd thin film and imprints. For cross-sectional SEM of PC substrate with Pd gratings, it was sputter coated with a thin film of Au (∼5 nm). The substrate was freshly cut with a pair of scissors and mounted for imaging. For performing transmission electron microscopy (TEM), a small portion of the Pd film was scratched and sonicated in toluene to make a dispersion of Pd nanoparticles, which was drop casted onto a holey carbon grid. The obtained Pd nanoparticles were characterized with a JEOL JEM-2100F high resolution transmission electron microscope operating at 200 kV.

Hydrogen Sensing. Metal contacts were drawn out of the Pd surface and patterns by means of silver paint for conducting electrical measurements. For blank sensors, the silver paint contacts were drawn on the edge of the film. On the other hand, for rigid and flexible sensors, gold electrodes were first deposited on the edge of the gratings. Silver paint contacts were then drawn from these electrodes from where electrical connections were made. Prior to sensing, the resistance of the Pd gratings was measured using a simple 4-probe set up (Loresta EP, MCP-T360). The sensing performance of the Pd film and gratings (on rigid or flexible substrates) was studied at room temperature by measuring the resistance change of the film when switching the sensing chamber environment from Ar to H_2 in a cyclic manner, with H_2 concentrations ranging from 50 to 3500 ppm. A homemade gas sensing setup with vacuum seals connected to air and H_2 (0.5%, He balance) gas cylinders was used. An electrical feedthrough was used to connect the sample to a Keithley 4200-SCS system. The sensing setup was coupled to corresponding mass flow controllers that provided variable H_2 concentration. Just before starting the sensing experiments, the whole system was pumped down with a roughing pump to 10^{-3} Torr to remove residual gases. The order of exposure at various H_2 concentrations was *randomized*. For example, the first sensing test was conducted at a hydrogen concentration of 509 ppm with other concentrations tested for subsequently in a random manner. Each concentration of the H_2 gas was flowed into the chamber for 90 s and was cut off for 120 s for recovery while flowing Ar gas (see the Supporting Information). The cycles were further repeated. The concentration of H_2 was controlled by mass flow controllers (MKS Instruments). A Keithley Semiconductor Characterization System model 4200-SCS was used to record current while sensing, which was then converted into resistance. All the sensing measurements were done in 2-probe geometry.

For hydrogen sensing with flexible sensor in the bent configuration, it was fixed at a bend angle of 90° (or at a radius of curvature = 3.57 mm) with the aid of a homemade screw setup (see Supporting Information). The sensor in bent configuration was kept inside the sensing chamber for measurements. For repeated flat, bent, and flat configuration measurements, the sensor was taken out after each measurement to change from one configuration to the other.

■ ASSOCIATED CONTENT

Ⓢ Supporting Information

Calculation for theoretical amount of Pd metal in PBM; summary of sensitivity and response time reported for H_2 sensors based on Pd thin films, nanowires and nanotubes including flexible Pd-based H_2 sensors in literature; XPS and roughness data of heat-treated Pd film; top-view SEM image of Pd lines embedded in a PC substrate; hydrogen sensing data in full range for flexible sensor in the bent configuration; sensitivity and response time definitions; baseline electrical properties of the imprinted palladium gratings; H_2 sensing in air using palladium gratings; arrangement of H_2 sensors (blank and flexible) for electrical measurements; and images of homemade screw setup for H_2 sensing using a flexible sensor in the bend configuration. This material is available free of charge via the Internet at http://pubs.acs.org.

■ AUTHOR INFORMATION

Corresponding Author

*E-mail: elehgw@nus.edu.sg, saifullahm@imre.a-star.edu.sg, kulkarni@jncasr.ac.in, radha.boya@northwestern.edu.

Present Address

[‖]Department of Materials Science and Engineering, Northwestern University, 2220 Campus Drive, Evanston, Illinois 60208, United States of America

Author Contributions

The manuscript was written through contributions of all authors. All authors have given approval to the final version of the manuscript.

Notes

The authors declare no competing financial interest.

■ ACKNOWLEDGMENTS

The authors would like to thank Dr. Zhi Han Lim for his assistance in the gas sensing setup. One of the authors (B.R.) would like thank the A*STAR for supporting her stay in Singapore as a visiting scholar at the Institute of Materials Research and Engineering. This work was supported by the NUS R-263-000-653/654-731/112 and IMRE-funded core project no. IMRE/09-1C0319. Additional support from Department of Science and Technology, India, is gratefully acknowledged.

■ REFERENCES

(1) Liekhus, K. J.; Zlochower, I. A.; Cashdollar, K. L.; Djordjevic, S. M.; Loehr, C. A. *J. Loss Prev. Process Ind.* **2000**, *13*, 377−384.

(2) Kay, B. D.; Peden, C. H. F.; Goodman, D. W. *Phys. Rev. B* **1986**, *34*, 817−822.

(3) Smith, R. J.; Otterson, D. A. *J. Phys. Chem. Solids* **1970**, *31*, 187−189.

(4) Pundt, A.; Kirchheim, R. *Annu. Rev. Mater. Res.* **2006**, *36*, 555−608.

(5) Lee, E.; Lee, J. M.; Koo, J. H.; Lee, T. *Int. J. Hydrogen Energy* **2010**, *35*, 6984−6991.

(6) Lewis, F. A. *The Palladium Hydrogen System*; Academic Press: New York, 1967.
(7) Butler, M. A. *Appl. Phys. Lett.* **1984**, *45*, 1007−1009.
(8) Maier, R. R. J.; Jones, B. J. S.; Barton, J. S.; McCulloch, S.; Allsop, T.; Jones, J. D. C.; Bennion, I. *J. Opt. A: Pure Appl. Opt.* **2007**, *9*, S45.
(9) Butler, M. A. *Sens. Actuators, B* **1994**, *22*, 155−163.
(10) Gupta, R.; Sagade, A. A.; Kulkarni, G. U. *Int. J. Hydrogen Energy* **2012**, *37*, 9443−9449.
(11) Cabrera, A. L.; Aguayo-Soto, R. *Catal. Lett.* **1997**, *45*, 79−83.
(12) Favier, F.; Walter, E. C.; Zach, M. P.; Benter, T.; Penner, R. M. *Science* **2001**, *293*, 2227−2231.
(13) Lee, J.; Shim, W.; Lee, E.; Noh, J.-S.; Lee, W. *Angew. Chem., Int. Ed.* **2011**, *50*, 5301−5305.
(14) Greco, F.; Ventrelli, L.; Dario, P.; Mazzolai, B.; Mattoli, V. *Int. J. Hydrogen Energy* **2012**, *37*, 17529−17539.
(15) Noh, J.-S.; Lee, J. M.; Lee, W. *Sensors* **2011**, *11*, 825−851.
(16) Sagade, A. A.; Radha, B.; Kulkarni, G. U. *Sens. Actuators, B* **2010**, *149*, 345−351.
(17) Kiefer, T.; Villanueva, L. G.; Fargier, F.; Favier, F.; Brugger, J. *Nanotechnology* **2010**, *21*, 505501.
(18) Xu, T.; Zach, M. P.; Xiao, Z. L.; Rosenmann, D.; Welp, U.; Kwok, W. K.; Crabtree, G. W. *Appl. Phys. Lett.* **2005**, *86*, 2031041.
(19) Joshi, R. K.; Krishnan, S.; Yoshimura, M.; Kumar, A. *Nanoscale Res. Lett.* **2009**, *4*, 1191−1196.
(20) Sun, Y.; Wang, H. H. *Adv. Mater.* **2007**, *19*, 2818−2823.
(21) Xie, B.; Liu, L.; Peng, X.; Zhang, Y.; Xu, Q.; Zheng, M.; Takiya, T.; Han, M. *J. Phys. Chem. C* **2011**, *115*, 16161−16166.
(22) Mubeen, S.; Zhang, T.; Yoo, B.; Deshusses, M. A.; Myung, N. V. *J. Phys. Chem. C* **2007**, *111*, 6321−6327.
(23) Kong, J.; Chapline, M. G.; Dai, H. *Adv. Mater.* **2001**, *13*, 1384−1386.
(24) Villanueva, L. G.; Fargier, F.; Kiefer, T.; Ramonda, M.; Brugger, J.; Favier, F. *Nanoscale* **2012**, *4*, 1964−1967.
(25) Yun, M.; Myung, N. V.; Vasquez, R. P.; Lee, C.; Menke, E.; Penner, R. M. *Nano Lett.* **2004**, *4*, 419−422.
(26) Im, Y.; Lee, C.; Vasquez, R. P.; Bangar, M. A.; Myung, N. V.; Menke, E. J.; Penner, R. M.; Yun, M. *Small* **2006**, *2*, 356−358.
(27) Jeon, K. J.; Jeun, M.; Lee, E.; Lee, J. M.; Lee, K.-I.; von Allmen, P.; Lee, W. *Nanotechnology* **2008**, *19*, 495501.
(28) Jeon, K. J.; Lee, J. M.; Lee, E.; Lee, W. *Nanotechnology* **2009**, *20*, 135502.
(29) Yang, F.; Kung, S.-C.; Cheng, M.; Hemminger, J. C.; Penner, R. M. *ACS Nano* **2010**, *4*, 5233−5244.
(30) Yu, S.; Welp, U.; Hua, L. Z.; Rydh, A.; Kwok, W. K.; Wang, H. H. *Chem. Mater.* **2005**, *17*, 3445−3450.
(31) Lim, M. A.; Kim, D. H.; Park, C.-O.; Lee, Y. W.; Han, S. W.; Li, Z.; Williams, R. S.; Park, I. *ACS Nano* **2012**, *6*, 598−608.
(32) Ksar, F.; Sharma, G. K.; Audonnet, F.; Beaunier, P.; Remita, H. *Nanotechnology* **2011**, *22*, 305609.
(33) Guo, L. J. *Adv. Mater.* **2007**, *19*, 495−513.
(34) Schrift, H. *J. Vac. Sci. Technol. B* **2008**, *26*, 458−480.
(35) Dumond, J. J.; Low, H. Y. *J. Vac. Sci. Technol. B* **2012**, *30*, 010801.
(36) Dinachali, S. S.; Saifullah, M. S. M.; Ganesan, R.; Thian, E. S.; He, C. *Adv. Funct. Mater.* **2013**, *23*, 2201−2211.
(37) Radha, B.; Lim, S. H.; Saifullah, M. S. M.; Kulkarni, G. U. *Sci. Rep.* **2013**, *3*, 1078.
(38) Yamauchi, M.; Ikeda, R.; Kitagawa, H.; Takata, M. *J. Phys. Chem. C* **2008**, *112*, 3294−3299.